A Decentralized Control Method for Direct Smart Grid Control of Refrigeration Systems*

Seyed Ehsan Shafiei[1], Roozbeh Izadi-Zamanabadi[1,2], Henrik Rasmussen[1] and Jakob Stoustrup[1]

***Abstract*— A decentralized control method is proposed to govern the electrical power consumption of supermarket refrigeration systems (SRS) for demand-side management in the smart grid. The control structure is designed in a supervisory level to provide desired set-points for distributed level controllers. No model information is required in this method. The temperature limits/constraints are respected. A novel adaptive saturation filter is also proposed to increase the system flexibility in storing and delivering the energy. The proposed control strategy is applied to a simulation benchmark that fairly simulate the CO_2 booster system of a supermarket refrigeration.**

I. INTRODUCTION

The growing demand for electrical energy and the increasing utilization of renewable energy sources create significant challenges for the power grid to provide a stable and sustainable supply of electricity. As part of the smart grid solutions, the consumption of electricity should be actively managed as well as the generation.

Demand response (DR) is a component of smart energy demand for managing costumer consumption of electricity. One strategy for DR implementation is real-time pricing [1] in which the load level of a consumer is optimized in response to electricity prices. Another strategy (considered for this study) is to directly manage the energy consumption of consumers. Implementation of such strategy requires at least two levels of design [2]: a higher level to dispatch the energy/power demand to consumers, and a lower level control design specific for each autonomous consumer providing balancing services. The latter is the focus of this paper.

Industrial refrigeration systems have been proven to be highly potential consumers for DR implementations [3]. Utilizing full DR potential of such consumers requires development of advanced control methods like model predictive control (MPC) [4]. Different MPC schemes have been proposed to minimize the cost of operation of refrigeration systems in smart grid. An economic-optimizing MPC scheme has been proposed by [5], where the objective function is formulated for cost minimization as well as peak load reduction. A complex nonlinear solver is employed and the local display case controllers are replaced by a centralized MPC. In [6] a MPC scheme has been designed in a supervisory control level. Two sets of set-point (*i.e.* pressure for suction manifold and temperatures for display cases) are separately calculated in different control loops and assigned to the distributed local controllers. A direct control implementation for multiple units of single vapor-compression cycle systems has been presented in [7]. An energy storage model is proposed and utilized by a predictive controller for implementation. The main reasons that MPC is widely used in such application are its mightiness at controlling multi-variable systems subject to constraints, and at incorporation of the model prediction in an optimal control problem.

Implementation of model-based controllers like MPC for supermarket refrigeration systems requires developing a high fidelity model which is itself a nontrivial and expensive procedure; especially considering the fact that the system dimension and configuration vary from one supermarket to another. Moreover, utilization of an optimizing controller for large-scale systems highly increases the complexity regarding the practical implementations. Nevertheless, the model-based controls are still valuable methods for investigating the full potential of demand response implementations.

In this paper, we propose a simple but efficient supervisory control structure including P and PI controllers that can enable balancing services of SRSs in smart grid. The heuristic algorithm proposed in [6] for the pressure set-point control is replaced by a proportional controller, and an *agility factor* is also introduced. Like [6], the supervisory controller (which is now simply a PI) assigns set-points to the air temperatures inside the cooling sites. No model information is required for the control implementation. The food temperatures should be constrained within the permissible limits. So we put a saturation filter at the control output that restricts the air temperature and consequently the food temperature. To handle windup problem due to the saturation filter, a decentralized structure equipped with anti-windup features is designed. In contrast to the MPC schemes, the model free controller cannot predict the future temperatures of the air and of the foodstuffs. So, to ensure the food safety, the same limits for the food temperatures should be considered for saturation limits applying to the air temperature. This however limits the range of control effort, and consequently decreases the control system flexibility in governing the power consumption. We have proposed an *adaptive saturation filter* that can effectively remove this restriction as well as respecting the food temperatures.

II. SYSTEM DESCRIPTION AND PROBLEM STATEMENT

In this section, we briefly explain a CO_2 booster configuration of a typical supermarket refrigeration system. Subse-

*This work is supported by the Southern Denmark Growth Forum and the European Regional Development Fund under the Project Smart & Cool.

[1]Section for Automation and Control, Department of Electronic Systems, Aalborg University, Aalborg, Denmark {ses, riz, hr, jakob} at es.aau.dk

[2]Danfoss A/S, 6430 Nordborg, Denmark {roozbeh} at danfoss.com

quently, the thermodynamics involving the cooling sites are introduced, and finally, the control problem is stated.

A. CO_2 Booster Refrigeration System

A basic layout of a typical refrigeration system including several display cases and freezing rooms with two compressor banks in a booster configuration is shown in Fig. 1. Starting from the receiver (REC), two-phase refrigerant (mix of liquid and vapor) at point '8' is split out into saturated liquid ('1') and saturated gas ('1b'). The latter is bypassed by a bypass valve (BPV), and the former flows into expansion valves where the refrigerant pressure drops to medium ('2') and low ('2′') pressures. The expansion valves EV_MT and EV_LT are responsible for regulating the air temperature inside the medium temperature (MT) and the low temperature (LT) cooling sites, respectively, by controlling the entering mass flow into the evaporators. Flowing through medium and low temperature evaporators (EVAP_MT and EVAP_LT), the refrigerant absorbs heat from the cold reservoir. The pressure of low temperature units (LT) is increased by the low stage compressor rack (COMP_LO). All mass flows from COMP_LO, EVAP_MT and BPV outlets are collected by a suction manifold at point '5' where the pressure is increased again by high stage compressors (COMP_HI). Afterward, the gas phase refrigerant enters the condenser to deliver the absorbed heat from cold reservoirs to the surrounding. The detailed thermodynamic analysis of such systems is described in [8].

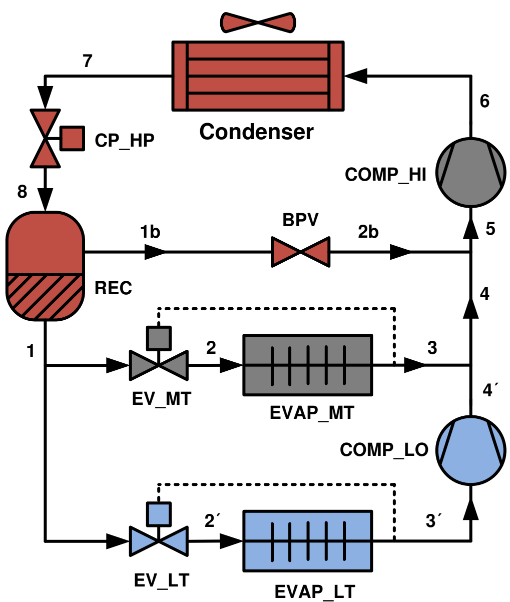

Fig. 1. Basic layout of a typical supermarket refrigeration system with booster configuration.

B. Cooling unit dynamics

The purpose of this subsection is to introduce the dynamical equations describing the thermodynamic processes involve the system. However, the model information are not used for the control design. The detailed modeling for such control applications have been explained in [13].

In the cold units (display cases and freezing rooms), heat is transfered from foodstuffs to cooled air, $\dot{Q}_{foods/air}$, and then from cooled air to circulated refrigerant, $\dot{Q}_e$, which the latter is also known as cooling capacity. There is however heat load from supermarket indoor, $\dot{Q}_{load}$, formulated as a variable disturbance. Here, we consider the measured air temperature entering the evaporator area as the cold unit temperature, T_{air}. Assuming a lumped temperature model, the following dynamical equations are derived based on energy balances for the mentioned heat transfers.

$$MCp_{foods}\frac{dT_{foods}}{dt} = -\dot{Q}_{foods/air} \tag{1}$$

$$MCp_{air}\frac{dT_{air}}{dt} = \dot{Q}_{load} + \dot{Q}_{foods/air} - \dot{Q}_e \tag{2}$$

where MCp denotes the corresponding mass multiplied by the heat capacity. The energy flows are

$$\dot{Q}_{foods/air} = UA_{foods/air}(T_{foods} - T_{air}), \tag{3}$$

$$\dot{Q}_{load} = UA_{load}(T_{indoor} - T_{air}), \tag{4}$$

and

$$\dot{Q}_e = UA_e(T_{air} - T_e) \tag{5}$$

where UA is the overall heat transfer coefficient, T_e is the evaporation temperature, and T_{indoor} is the supermarket indoor temperature. The heat transfer coefficient between the refrigerant and the display case temperature, UA_e, is described as a linear function of the mass of the liquefied refrigerant in the evaporator [9],

$$UA_e = k_m M_r, \tag{6}$$

where k_m is a constant parameter. The refrigerant mass, $0 \leq M_r \leq M_{r,max}$, is subject to the following dynamic [10],

$$\frac{dM_r}{dt} = \dot{m}_{r,in} - \dot{m}_{r,out}, \tag{7}$$

where $\dot{m}_{r,in}$ and $\dot{m}_{r,out}$ are the mass flow rate of refrigerant into and out of the evaporator, respectively. The entering mass flow is determined by the opening degree of the expansion valve and is described by the following equation:

$$\dot{m}_{r,in} = OD\ KvA\sqrt{2\rho_{suc}(P_{rec} - P_e)} \tag{8}$$

where OD is the opening degree of the valve with a value between 0 (closed) to 1 (fully opened), P_{rec} and P_e are receiver and suction manifold (evaporating) pressures, ρ_{suc} is the density of the circulating refrigerant, and KvA denotes a constant characterizing the valve. The leaving mass flow is given by

$$\dot{m}_{r,out} = \frac{\dot{Q}_e}{\Delta h_{lg}} \tag{9}$$

where Δh_{lg} is the specific latent heat of the refrigerant in the evaporator, which is a nonlinear function of the suction pressure. When the mass of refrigerant in the evaporator reaches its maximum value ($M_{r,max}$), the entering mass flow is equal to the leaving one.

C. Problem Statement

In framework of the direct smart grid control, the SRS is supposed to follow a power reference assigned by the aggregator. Here the problem is to design a control structure enabling the SRS to regulate its electrical power consumption by storing and delivering energy into and out from the existing thermal masses in cooling sites.

The practical issues are, first, we do not use any model information in our control practice, and second, we do not replace the existing local distributed controllers in the system.

III. Design of Control Structure

In order to keep the local distributed controllers at their places, the smart grid control scheme should be implemented in a supervisory level with an outer control loop including the closed-loop system. There are two sets of control variables to which the supervisory controllers can assign set-points: the suction pressure, and the air temperatures circulating inside the cooling sites.

A. Pressure Set-Point Control

The coupling variable between the cooling units is the suction pressure. If it was possible to assign the pressure set-points disregarding the cooling air temperatures, then we could apply the temperature set-point to each unit decoupled from the other ones. A simple minded method is to assign a constant pressure set-point that is low enough to support the cooling capacity required for low temperatures. But this will increase the power consumption in a normal operation.

A near optimal algorithm was designed in [6] by which the pressure set-point is changed such that always one of the expansion valve is kept fully opened. Here we apply such optimality by designing a simple proportional controller with saturation limits (to respect the pressure constraints). In order to prevent a large proportional gain and consequently a large variation of the set-point, the control command is considered as the change of set-point,

$$\Delta P_{ref} = K_p(r_{OD} - \overline{OD}_{max}) \tag{10}$$

where K_p is the proportional gain, $\overline{OD}$ is the vector of opening degree of the valves, and $\overline{OD}_{max}$ corresponds to the maximum element of it. $r_{OD} = 1 - \varepsilon$ is the maximum value that the fully open valve should follow. It should be a little bit smaller than 1, because the optimality hypothesis is to keep only one valve fully opened.

Remark 1: The larger ε, the larger gain is applied while decreasing the pressure. This can increase the flexibility considering the rate of change of the temperatures. So that ε is called *agility factor*. It means when the system is demanded to store energy by decreasing the cooling site temperatures, it can respond more agile with a larger ε. On the other hand, the optimal condition corresponds to $\varepsilon = 0$. So there is a *trade-off* between the flexibility and the optimality.

The control command (10) is then added to the pressure feedback to form the applied set-point,

$$P_{ref} = \Delta P_{ref} + P_e. \tag{11}$$

In order to respect the pressure limits, this set-point is passed through a saturation filter before applying to the system. The saturation filter is given by the following relation.

$$\text{sat}(u) = \begin{cases} u_{max} & u \geq u_{max} \\ u & u_{min} < u < u_{max} \\ u_{min} & u \leq u_{min} \end{cases} \tag{12}$$

Fig. 2 shows the designed structure for set-point control of the suction pressure.

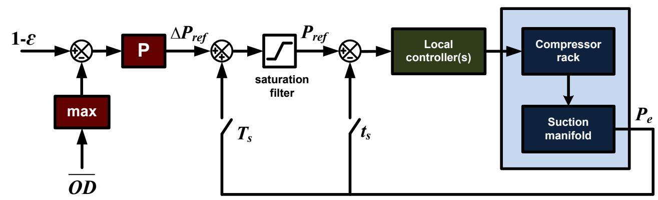

Fig. 2. Control structure for set-point control of the suction pressure. The local controllers use a very shorter sampling period (t_s) than of the supervisory P controller (T_s).

Remark 2: The local controller in Fig. 2 regulates the suction pressure to the assigned reference within the operating range. There are also superheat controllers governing the valve opening degrees to ensure the refrigerants exiting the evaporators are completely vaporized. The saturation filter is imposed to guarantee that the pressure set-point does not exceed the range of operations of the local pressure controller as well as the distributed superheat controllers. Therefor, the transfer function from P_{ref} to P_e describes a stable close loop system. In practice, the settling time of the inner closed loop system is less than one minute. So, by considering the sampling time larger than one minute for the outer supervisory loop, and assuming a perfect regulation, the transfer function of the inner closed loop system would be a unit delay which means $P_e[k] = P_{ref}[k-1]$.

B. Temperature Set-Point Control

This section proposes a supervisory control structure for set-point control of the air temperatures of the cooling sites. The main idea is to regulate the electrical power consumption of the compressors by changing these temperature set-points. So that in case of increasing the power above the base-line — decided by the aggregator — the control system starts storing energy in cooling sites, and vice versa.

Fig. 3 illustrates the designed control structure. Because of the food safety, there are strict limits on variation range of the food temperatures. The local controllers operating on the valves control the air temperature inside the cold storages (see (1)). Since the food temperature (due to a higher heat capacity) cannot vary larger than the air temperature, applying the same limits on the air temperatures can guarantee the limits on the food temperatures as well (see (2)). The constraints are applied by putting the saturation filters with the following saturation bounds at the output of the ith PI controller.

$$\overline{U}_i = (\overline{T}_i - T_{0,i}), \tag{13}$$

and

$$\underline{U}_i = (\underline{T}_i - T_{0,i}), \tag{14}$$

where $\overline{T}$ and $\underline{T}$ are respectively the upper and lower limits of the food temperature, and T_0 is the fixed set-point for normal operation (that is when the system is not under the direct control feedback loop).

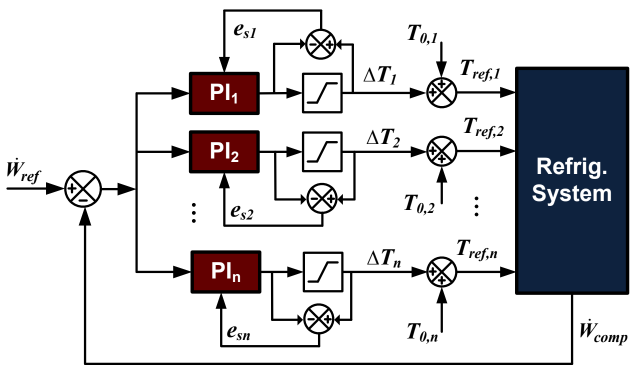

Fig. 3. Control structure for set-point control of the air temperatures in cooling sites.

The supervisory controllers apply the set-point change ΔT_i to each unit. Then this control command is added to a fixed set-points $T_{0,i}$ to form the temperature reference ($T_{ref,i}$) for the ith unit.

$$T_{ref,i} = \Delta T_i + T_{0,i} \tag{15}$$

The advantages of designing decentralized structure for supervisory PIs instead of designing a single PI with distributed weighting factors (gains) are explained as follows. The first reason is that this structure leaves two degrees of freedom in designing the controller for each cooling site. This can however facilitate the future investigations to find the optimum controller parameters. The second and the most important reason is that because of the saturation filters, the integral term will windup once the control effort reaches the limits. The anti-windup feature can be easily supported by this decentralization.

The error feedbacks $e_{s,i}$ go to the PI controllers in Fig. 3 are required for the anti-windup design as explained in [11]. A sample PI unit including the anti-windup feature is shown in Fig. 4.

Putting as the same constraints on the air temperatures as the food temperatures cuts down the demand response ability of the system from the speed of response point of view. In model-based designs like MPC, this can be easily handled by just putting the constraints on the food temperatures that is honored by the prediction of the future states/outputs. In case of lack of the model, there is no specific solution for such problems. The next section proposes a novel method that can deal with the problem by replacing the fixed saturation filters by adaptive ones.

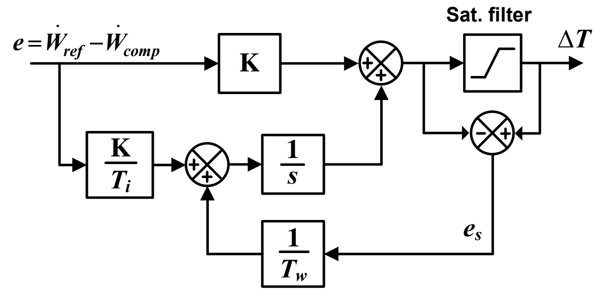

Fig. 4. PI controller with anti-windup.

C. Adaptive Saturation Filter

In the proposed adaptive saturation filter, the saturation limits are adaptively updated based on the current value of the food temperature. Each PI unit in the control structure of Fig. 3 should be updated to the one shown in Fig. 5.

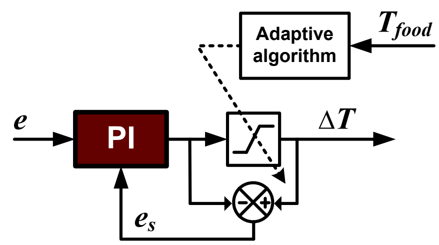

Fig. 5. PI controller with anti-windup and adaptive saturation filter.

The adaptive algorithm for updating the saturation limits is described by

$$u_{max,i}(t) = \overline{U}_i + K_{u,i}(\overline{T}_i - T_{foods,i}(t)), \tag{16}$$

and

$$u_{min,i}(t) = \underline{U}_i + K_{l,i}(\underline{T}_i - T_{foods,i}(t)), \tag{17}$$

where $K_{u,i}$ and $K_{l,i}$ are constant parameters defined as *saturation limit gains*. The right-hand side of the above equations are the adaptive terms added to (13) and (14). For the rest of this section we discuss some features of the designed filter considering (16); the similar discussion can be also made for the case of (17). For example consider the case that the food temperature is below of its maximum limit ($T_{foods,i} < \overline{T}_i$) and we want to increase it to deliver the storage. At this time, depending on the saturation limit gains, a higher saturation limit is applied by the filter that lets the air temperature goes to a higher level. The higher air temperature ($T_{air} > T_{foods}$), the higher absolute value of $\dot{Q}_{foods/air}$ is applied to (2) that can govern the food temperature more effectively. While T_{foods} approaching its limit, the saturation limit decreases until once the food temperature touches the limit, the adaptive term in (16) will disappear.

Remark 3: The adaptive saturation filter can compensate the disturbance effect more efficient than the fixed parameter filter. In case of violation of the upper temperature limit due to a large disturbance, the adaptive term in (16) becomes negative that makes the saturation limit tighter than of

(13). It means that a larger input gain is applied to the food temperature dynamics in the opposite direction of the disturbance effect.

Remark 4: The value of the saturation limit gains (K_u or K_l) can be specified by considering the rate of change of the food temperature. Taking the first derivative of (16) gives

$$\frac{u_{max,i}}{dt} = -K_{u,i}\frac{T_{foods,i}}{dt}. \tag{18}$$

So, for instance if $K_u = 1$, the saturation limit changes with the same rate of the food temperature.

IV. Simulation Results

In this section, the proposed method is applied to a supermarket refrigeration system including 7 MT display cases and 4 LT freezing storages [12], [13]. Each cooling unit is equipped with a local PI controller regulating the air temperature inside the unit to the assigned set-point.

A. Normal operation

In normal operation the system is not in the closed-loop smart grid control. The temperature limits for food safeties are $\overline{T} = 3.5$ °C and $\underline{T} = 0.5$ °C for the MT sites, and $\overline{T} = -19$ °C and $\underline{T} = -25$ °C for the LT sites. The temperature set-points are set fixed to the upper limits to minimize the energy consumption.

1) Fixed pressure set-point: The suction pressure set-point is set to $P_{ref} = 24$ bar that can provide the pressure low enough to cool the air temperature down to the lower limit in case of necessity. Total electrical power consumption of the compressor racks with this set-up are shown in Fig. 6(a) with dotted line.

2) Pressure set-point control: At this step we apply the pressure set-point control using (10) and (11). The pressure limits are $\underline{P}_e = 20$ bar and $\overline{P}_e = 31$ bar. The proportional gain and the agility factor are set to $K_p = 5$ and $\varepsilon = 0.1$, respectively. As can be seen from Fig. 6(a), the base-line of the power consumption in normal operation is decreased by applying the pressure control method. The suction pressure is also shown in Fig. 6(b).

In a period of 24 hours, the power reference scenario is such that the aggregator demands the base-line power consumption until 5:00 AM. Following that, it demands an increase up to 20% over the base-line for 5:00-15:00, and a reduction down to 20% below the base-line for 15:00-20:00. Finally the reference gets back to the base-line for 20:00-24:00 to be ready for demand response for the next day. In the sequel, different responses by different controls are compared and the results are shown in a single plot.

B. Centralized control

The centralized control has the same feedback structure as Fig. 3 but includes only one centralized PI controller. The controller gain and integration time are $K = 0.1$ and $T_i = 30$ for both MT and LT units. The result is shown in Fig. 7 where the response to this control is depicted by dotted line. During the the increase period, saturation limits are not reached, so the controller can fairly increase the power. But

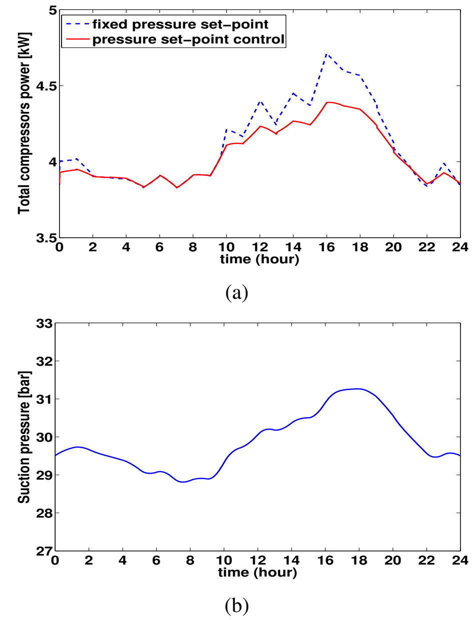

Fig. 6. Simulation results for normal operation. (a) The base-line of the electrical power consumptions of the compressor racks gets lower by applying the proposed pressure set-point control method. (b) The suction pressure after applying the control method.

it cannot decrease the power enough during the reduction demand because of activation of the saturation limits. After the reduction period, because of the integrator windup the centralized controller is also not able to regulate the power back to the base-line.

C. Decentralized control

In order to have a fair comparison, the same gain and integration time as the centralized control are considered for each decentralized PI controller. The anti-windup gain [11] is $T_w = 0.5T_i$. Now the controller can regulate the power back to the base-line after the reduction period where the saturation limits were activated.

D. Adaptive saturation filter

Fig. 8 shows the air and food temperatures of one of the LT display cases after applying the adaptive saturation filter. The trends are similar for the other cooling sites. The adaptive saturation filter lets the air temperature goes above the limit and while the food temperature is getting close to it, the air temperature is decreased adaptively. So the food temperature limits are not violated using this method. As a result, the power consumption can be decreased effectively during the reduction period as illustrated in Fig. 7. This result shows the superiority of the proposed method in delivering the stored energy. The same argument is also valid in case of storing energy when a higher increase of power is demanded that can lead to activation of the lower saturation limits for the temperature set-points.

V. Discussions

It should be noted that our purpose here is not a perfect power following control. The perfect power reference track-

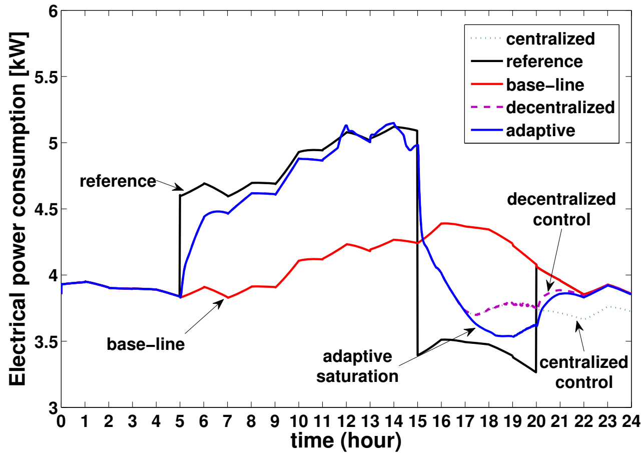

Fig. 7. Electrical power consumption of the compressor racks in case of centralized control (dotted), decentralized control (dashed), and decentralized control with adaptive saturation filter (solid).

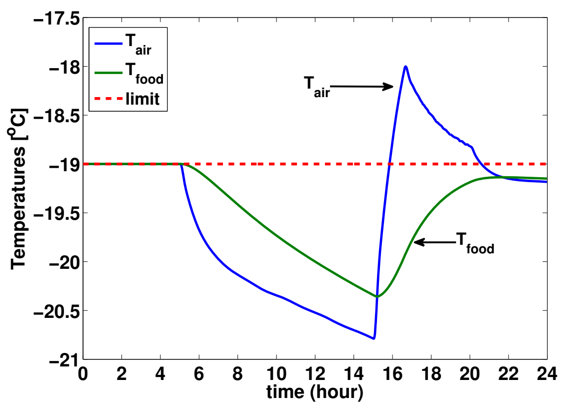

Fig. 8. The air and food temperatures for one of the LT display cases. The trends are similar for the other display cases.

ing can be obtained by directly controlling the compressor speeds. But it does not necessarily mean that we are storing energy in display cases during the increase period. On the other hand, just turning off the compressors during the reduction period can make problems in the high pressure CO_2 systems. By applying the mentioned power reference we could analyze the control response in case of a likely upward and downward power demands.

The LT cooling sites due to better isolations and consequently less disturbance loads are better candidate to be employed in the balancing services than the MT sites. Because of the booster configuration (Fig. 1) the low stage compressors corresponding to LT units have a lower capacity than the higher stage compressors. By applying the same control gain to both LT and MT units (as we did here) the low stage compressors are more excited than of the higher stage that means the LT units will be more involved in the balancing services that is a desired objective.

The optimal gains for the proposed controllers can be obtained using an accurate model, or by designing some data-driven experiments to tune the gains. Addressing this issue is however out of the scope of the current paper. Heuristically, the display cases with larger existing thermal masses and better isolations should be assigned more gains for their decentralized controllers.

VI. Conclusion

A new control structure including P and PI controllers for direct control of refrigeration systems in smart grid was proposed. No model information is required for the control implementation. The control was designed in a supervisory level to provide desired set-points to the local distributed controllers. Two different control loops were designed for decoupling the pressure set-point control from the temperature set-point control. In order to respect the temperature constraints, and at the same time avoiding windup problem, a decentralized control method was proposed. A new adaptive scheme for the saturation filter was designed to utilize the most potential of energy storages in the cooling sites. This is a new control structure for this specific application that leaves the possibility of further improvements and developments for the future works.

References

[1] A. J. Conejo, J. M. Morales, and L. Barino, "Real-time demand response model," *IEEE Transactions on Smart Grid*, vol. 1, no. 3, pp. 236–242, 2010.

[2] K. Trangbaek, J. D. Bendtsen, and J. Stoustrup, "Hierarchical control for smart grids," in *Proceedings of the 18th IFAC World Congress*, (Milan, Italy), IFAC, Aug. 2011.

[3] S. Goli, A. McKane, and D. Olsen, "Demand response opportunities in industrial refrigerated warehouses in california," in *2011 ACEEE Summer Study on Energy Efficiency in Industry*, (Niagara Falls, NY, USA), July 2011.

[4] T. Hovgaard, L. Larsen, K. Edlund, and J. Jørgensen, "Model predictive control technologies for efficient and flexible power consumption in refrigeration systems," *Energy*, vol. 44, pp. 105–116, 2012.

[5] T. G. Hovgaard, L. F. S. Larsen, and J. B. Jørgensen, "Flexible and cost efficient power consumption using economic mpc: A supermarket refrigeration benchmark," in *50th IEEE Conference on Decision and Control and European Control Conference*, (Orlando, Florida, USA), Dec. 2011.

[6] S. E. Shafiei, J. Stoustrup, and H. Rasmussen, "A supervisory control approach in economic mpc design for refrigeration systems," in *European Control Conference (Accepted paper)*, (Zürich, Switzerland), July 2013.

[7] R. Pedersen, J. Schwensen, S. Sivabalan, C. Corazzol, S. E. Shafiei, K. Vinther, and J. Stoustrup, "Direct control implementation of a refrigeration system in smart grid," in *American Control Conference (Accepted paper)*, (Washington DC, USA), June 2013.

[8] Y. T. Ge and S. A. Tassou, "Thermodynamic analysis of transcritical co_2 booster refrigeration systems in supermarket," *Energy Conversion and Management*, vol. 52, pp. 1868–1875, 2011.

[9] D. Sarabia, F. Capraro, L. F. S. Larsen, and C. Prada, "Hybrid nmpc of supermarket display cases," *Control Engineering Practice*, vol. 17, pp. 428–441, 2009.

[10] L. N. Petersen, H. Madsen, and C. Heerup, "Eso2 optimization of supermarket refrigeration systems," tech. rep., Technical University of Denmark, Department of Informatics and Mathematical Modeling, 2012.

[11] K. J. Åström and T. Hägglund, *Advanced Pid Control*. ISA-The Instrumentation, Systems, and Automation Society, 2006.

[12] "SRSim: A simulation benchmark for supermarket refrigeration systems using matlab." `http://www.es.aau.dk/projects/refrigeration/simulation-tools/`, Feb. 2013.

[13] S. E. Shafiei, H. Rasmussen, and J. Stoustrup, "Modeling supermarket refrigeration systems for demand-side management," *Energies*, vol. 6, no. 2, pp. 900–920, 2013.